FAST AND CONTROLLABLE ELASTOCAPILLARY FLOW CHANNELS USING SUSPENDED MEMBRANES

Sam J. Fishlock[1], David Steele[1], Srinivasu V. Puttaswamy[1], Gennady V. Lubarsky[1], Cesar Navarro[1], William P. Burns[1] and James McLaughlin[1]

Connected Health Innovation Centre, Engineering Research Institute, Ulster University, Newtownabbey, United Kingdom.

ABSTRACT

The ability to control the fluid velocity and flow rate in microfluidic paper-based analytical devices (µPADS) will help to enable more sensitive and flexible point-of-care (POC) diagnostics. We present an elastocapillary channel design, for fluid flow in porous membranes, which enables an increase in flow velocity by a factor of up to 4.45 compared with a porous membrane used in a standard, non-suspended, format. The increase in flow rate is controllable with varying channel width, and is enabled by using an elastocapillary action, where the flexible porous membrane is suspended over a rigid substrate and deformed during fluid imbibition. This enabling technology is particularly useful in POC diagnostics, where small samples need be rapidly transported and mixed with minimal loss of volume.

INTRODUCTION

Diagnostic µPADS based on porous fluidic networks, primarily from substrates such as filter paper [1] or nitrocellulose membranes [2] are attractive for low-cost diagnostic applications, for example where access to healthcare is low due to poverty, or where people reside in inaccessible locations. The portability and ease of use of such devices also makes µPADS attractive in higher-income situations, but where the patient may wish not to visit a healthcare facility and thereby save time.

Compared to traditional lab-based ELISA-type diagnostic kits or polymer-based microfluidic devices, porous substrate-based devices are often low in cost, however to have a greater impact in healthcare their sensitivity and functionality will need to be increased. In particular, the design of the fluid channels will be an important means to address these issues. Specifically, the ability to control the flow rate in porous microfluidic channels is useful in a number of applications.

Slowing down fluid flow has been used to increase the available incubation time for reagent mixing, and thus increase the sensitivity in diagnostic tests for detecting Human IgG antibodies [3] and also as a method of timing reagent delivery [4]. Slowing fluid flow has been achieved using various methods such as printed wax pillars [3], using absorbing shunts [4] and dissolved sucrose [5]. These methods enable limited control of the flow rate in porous channels, however since they act solely by slowing the flow rate, this limits usage when rapid analysis is required and may also lead to loss of sample through evaporation [6].

Tools for speeding up the fluid flow in porous networks are also very attractive since they can enable fluid to move into a reaction area more quickly and reduce overall analysis time. Fast flow channels have been fabricated in various methods such as using double-stacked paper channels [7] and patterning open channels using a craft cutter in paper substrates [8].

Fundamental analysis of fluid mechanics systems have shown [9]–[11] that the meniscus rise of fluid between one rigid and one flexible sheet can rise indefinitely, overcoming the normal equilibrium (Jurin) height. This meniscus rise is due to a flexible sheet deforming under capillary force, toward the rigid sheet, creating an infinitesimal gap between the two surfaces. This elastocapillary principle has been used in a microfluidic device [12], where a porous filter paper substrate was sandwiched between two polyester flexible cover-slips, increasing flow velocity. This increase in flow velocity gave increased sensitivity in detecting pesticide, as liquid flowed more rapidly into an incubation area for longer incubation time. However, this design is limited in controlling flow (for example minimising fluid volume) since the width of the fast-flow channel is defined by the width of the flexible coverslip, which may not easily be altered along the channel length. The complexity of fabricating a 3-tiered structure also reduces the attractive simplicity of µPADS.

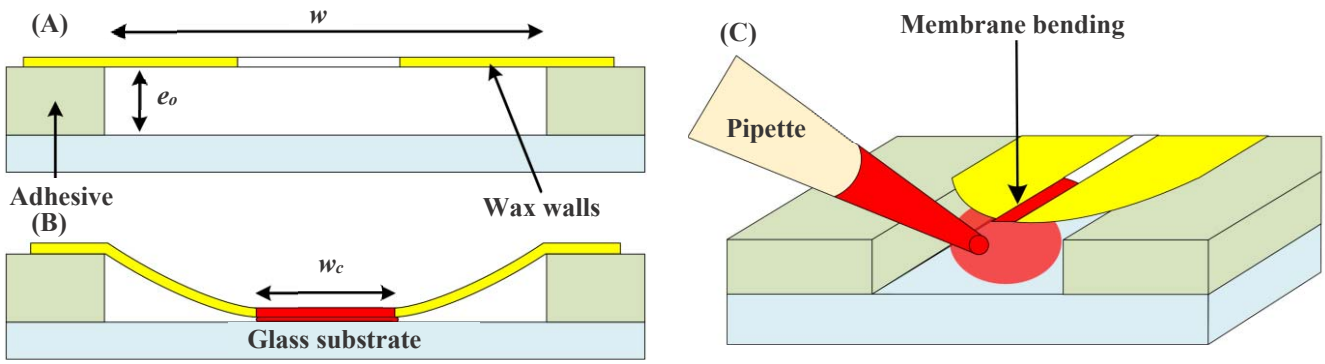

Figure 1 (A) Diagram of the cross section of the elastocapillary channel. (B) Channel deformation during elastocapillary imbibition. (C) Diagram showing how fluid is loaded onto the channel end.

In this work, we present the design, fabrication and analysis of an elastocapillary channel, using wax-printed nitrocellulose membranes. Development of nitrocellulose membranes is particularly attractive in applications where very low volumes of liquid are available, or desirable, for example a blood sample for POC diagnostics. The advantages of nitrocellulose include its low thickness (~ 120 µm) which means little liquid is lost in void volume, well characterised flow and potential for antibody immobilisation. The design is very simple to fabricate, whereby the nitrocellulose membrane is itself used as the flexible sheet in an elastocapillary system. The design comprises a nitrocellulose membrane with a wax printed channel, suspended over a glass substrate using a double-sided adhesive.

METHODOLOGY

Design of elastocapillary channel

Elastocapillary action occurs when a capillary force deforms an elastic material. In this example, the capillary force between the suspended membrane and the substrate is used to deflect the membrane. We note that the characteristic capillary length in this system is small (the membrane is effectively stuck down to the substrate [10]) and consequently has a small Bond number, and any gravitational effects can be ignored in this system. Figure 1 shows a schematic cross section of the channel used in this work. The membrane will undergo bending (the membrane will be pulled downward towards the glass substrate) if the surface energy ε_γ is high enough to overcome the elastic bending energy ε_B of the membrane. The surface energy may be calculated as:

$$\varepsilon_\gamma = 2\gamma w_c \tag{1}$$

Where γ is the surface tension of water, w_c is the width of the defined channel, since the liquid is confined in this region. The bending energy of the membrane is:

$$\varepsilon_B = \frac{3}{2}\frac{Be_0^2}{w^3} \tag{2}$$

Where B is the bending stiffness of the membrane, e_o is the suspended height above the glass substrate and w is the total suspended width. The energy ε_t of the system for a horizontal channel is thus:

$$\varepsilon_t = -\varepsilon_\gamma + \varepsilon_B \tag{3}$$

For elastocapillary imbibition to take place, the surface energy must overcome the bending energy. The values of geometry (e_0 = 60 µm, w = 4.0 mm , w_c is 0.45 to 2.4 mm) yield $\varepsilon_\gamma >> \varepsilon_B$ (ε_γ = ~ 49 to 259 µJ vs. ε_B = ~ 12 µJ) and this ensures that elastocapillary imbibition can take place in all fabricated channels.

The elastocapillary action effectively produces a thin microchannel between the membrane and the substrate of width w_c. Yang *et al.* [13] described the position of the front of the capillary meniscus, over time, $x(t)$ in a microchannel:

$$x(t) = \sqrt{Dt}, D = \left(\frac{h(\gamma_{sa} - \gamma_{sl})}{2\mu}\right) \tag{4}$$

Where D is diffusion coefficient and h is the characteristic length, γ_{sa} and γ_{sl} are surface tension between substrate-air and substrate-liquid, respectively. μ is dynamic viscosity.

Fabrication of elastocapillary channel

The elastocapillary channel comprises a patterned nitrocellulose membrane (Whatman AE99, 8 µm pore-size) which is suspended over a glass substrate. To fabricate the structure, uniform-width channels of width between 0.6 and 2.4 mm were defined in the membrane using wax printing (Xerox ColorQube 8580N) and then melted at 125 °C on a hotplate for 5 minutes. The substrate is prepared by covering a glass slide in double-side adhesive (ARcare 8570, 60 µm thickness) and laser patterning (VLS 230, Universal Laser) a 4.0 mm wide channel in the adhesive, which is peeled off of the glass substrate to create the suspended region as shown in Figure 1(A). The porous membrane is suspended over the glass substrate, and used as the flexible sheet in the elastocapillary system, shown in Figure 1(B). The channel is aligned to the centre of the suspended section by using two laser-marked scribes on the top side of the adhesive layer.

To demonstrate the ability to control the flow rate a channel of variable width, with discrete channel widths of (0.45, 1.20 and 2.46 mm) was fabricated.

RESULTS AND DISCUSSION

To measure the flow of liquid through the elastocapillary system, 15 µL of water (containing 1% v/v red (Wilton) food colouring) was pipetted onto one end of the flow channel as shown in Figure 1 (C). The imbibition of the liquid into each channel was measured using a digital video camera, and the distance travelled of the liquid front was measured at set time points. The results are shown in Figure 2, comparing the liquid front position of varying width suspended channels and non-suspended channels of 0.7 to 2.4 mm width and with a visual comparison shown in Figure 3. A marked increase in the flow velocity is observed when the channels are suspended. After 5 seconds, the 2.4 and 0.7 mm width channels, respectively show 4.45 and 1.97 factor increase in liquid front position over the non-suspended channels.

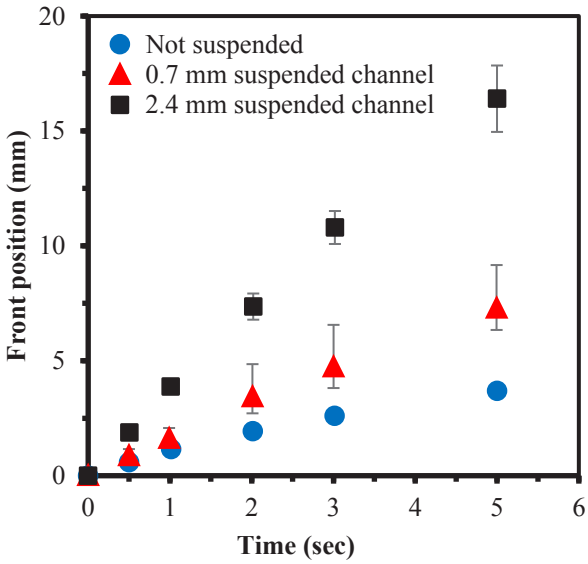

Figure 2. Position of the liquid front over time in suspended elastocapillary channels of 0.7 and 2.4 mm compared with non-suspended channels

A channel of variable width (3 discreet regions of 0.45, 1.20 and 2.46 mm) was also fabricated (visible in Figure 4 inset), and the flow velocity in each region was measured, decreasing by 29 % and 79 % as the channel width is decreased, as shown in Figure 4.

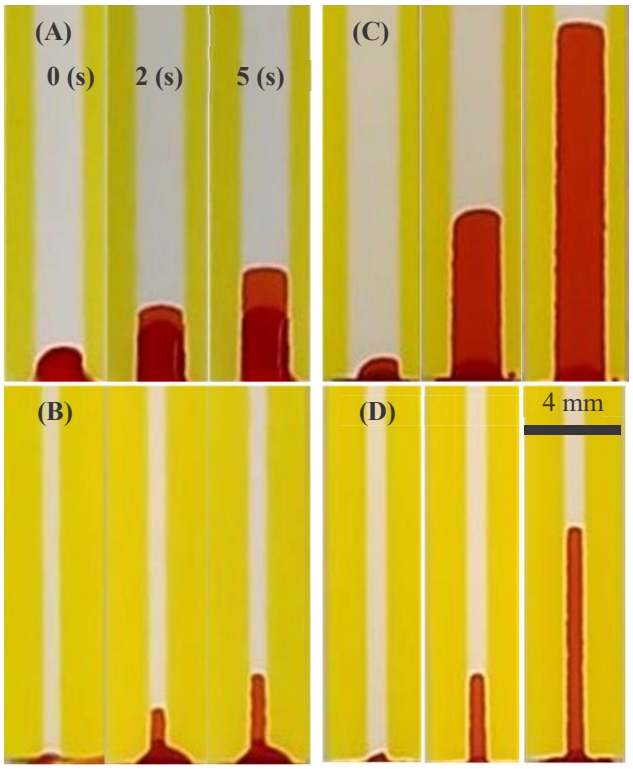

Figure 3. Video stills after 0,2.0 and 5.0 seconds of liquid imbibition into non-suspended (A, B) and suspended (C, D) channels 2.4 (A, C) and 0.7 mm width (B, D).

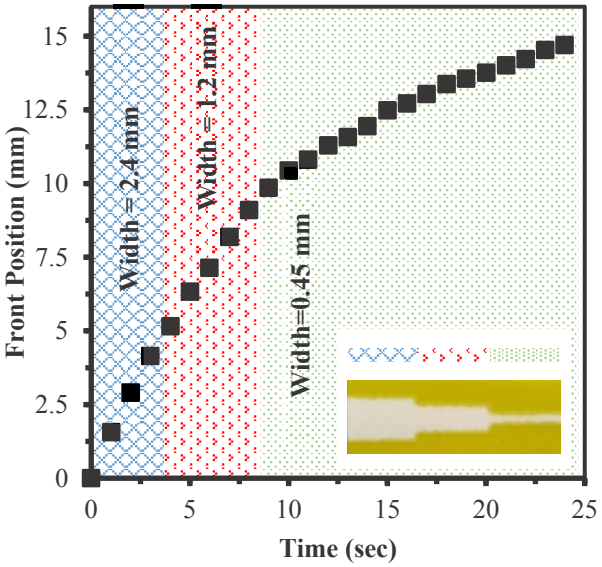

Figure 4. Liquid front position over time in an elastocapillary channel of controlled width from 0.45 to 2.46 mm. (Inset) image of variable width channel.

The flow velocity in non-suspended variable width channels is not largely affected by the width of the channel, when moving from larger to smaller channels [14], whereas in the suspended channel, the flow demonstrably slows as it enters each narrower section.

Furthermore, for single (constant) width channels, the flow velocity in non-suspended channels is not affected by width (in wet-out flow). This is visible in Figure 3 (A,B) where the meniscus fronts in channels of 0.7 and 2.4 mm width flow at the same velocity. However we have measured the front position over time of a number of suspended channels (width 0.60 to 2.48 mm), and show in Figure 5 that the meniscus front position $x(t)$ follows time$^{1/2}$ and the square root of channel width $w_c^{1/2}$ linearly; which demonstrates that the flow dynamics in this channel follow the behaviour described in Equation (4). We note that the x vs. time$^{1/2}$ flow velocity is similar to the behaviour observed in two-ply channels by Martinez *et al.* [7].

The wide range of flow velocity achieved with relatively small changes in channel width demonstrates that elastocapillary channels are a simple method of controlling fluid velocity in µPADS, which is greatly useful in POC devices where precise reagent mixing time is required.

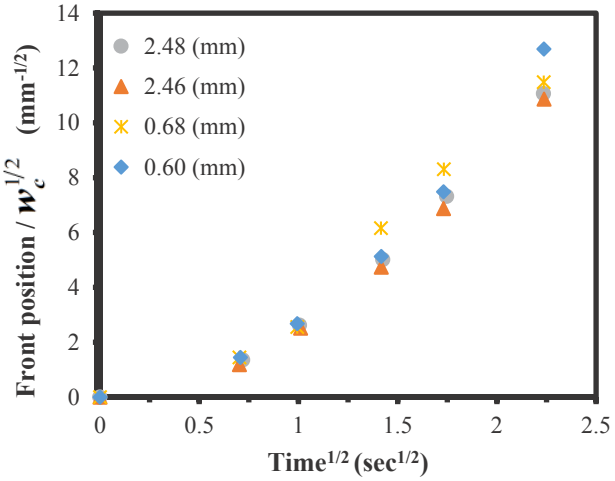

Figure 5. Liquid front position divided by $w_c^{1/2}$ plotted against the square root of time in suspended channels of varying width between 0.60 and 2.48 mm.

CONCLUSIONS

In this work we have shown the design, fabrication and characterisation of fast flow channels using the elastocapillary action, by suspending nitrocellulose membranes over glass substrates. Using the elastocapillary effect enables an increase in fluid velocity, here demonstrated at a 4.45 factor increase over the velocity in a non-suspended nitrocellulose membrane.

The channel design also enables the velocity to be controlled by altering the width of the patterned channel; with a clear increase in the flow velocity with wider channels, which follows the width relationship of the channel according to $w_c^{1/2}$. This controllability helps in the design of low-fluid-volume µPADS in particular.

ACKNOWLEDGEMENTS

We gratefully acknowledge the funding under the Heart Failure project from Invest Northern Ireland under the Connected Health Innovation Centre (CHIC) competence centre.

REFERENCES

[1] A. W. Martinez, S. T. Phillips, M. J. Butte, and G. M. Whitesides, "Patterned paper as a platform for inexpensive, low-volume, portable bioassays," *Angewandte Chemie - International Edition*, vol. 46, no. 8, pp. 1318–1320, 2007.

[2] Y. Lu, W. Shi, J. Qin, and B. Lin, "Fabrication and characterization of paper-based microfluidics prepared in nitrocellulose membrane by Wax printing," *Analytical Chemistry*, vol. 82, no. 1, pp. 329–335, 2010.

[3] L. Rivas, M. Medina-Sánchez, A. de la Escosura-Muñiz, and A. Merkoçi, "Improving sensitivity of gold nanoparticle-based lateral flow assays by using wax-printed pillars as delay barriers of microfluidics.," *Lab on a chip*, vol. 14, no. 22, pp. 4406–14, 2014.

[4] B. J. Toley, B. McKenzie, T. Liang, J. R. Buser, P. Yager, and E. Fu, "Tunable-Delay Shunts for Paper Micro fluidicDevices," *Analytical chemistry*, vol. 85, no. 23, pp. 11545–52, 2013.

[5] B. Lutz, T. Liang, E. Fu, S. Ramachandran, P. Kauffman, and P. Yager, "Dissolvable fluidic time delays for programming multi-step assays in instrument-free paper diagnostics," *Lab on a Chip*, vol. 13, no. 20, p. 4004, 2013.

[6] C. Renault, J. Koehne, A. J. Ricco, and R. M. Crooks, "Three-dimensional wax patterning of paper fluidic devices," *Langmuir*, vol. 30, no. 23, pp. 7030–7036, 2014.

[7] C. K. Camplisson, K. M. Schilling, W. L. Pedrotti, H. A. Stone, and A. W. Martinez, "Two-ply channels for faster wicking in paper-based microfluidic devices," *Lab Chip*, vol. 15, no. 23, pp. 4461–4466, 2015.

[8] D. L. Giokas, G. Z. Tsogas, and A. G. Vlessidis, "Programming fluid transport in paper-based microfluidic devices using razor-crafted open channels," *Analytical Chemistry*, vol. 86, no. 13, pp. 6202–6207, 2014.

[9] J. Bico, B. Roman, L. Moulin, and A. Boudaoud, "Adhesion: Elastocapillary coalescence in wet hair," *Nature*, vol. 432, no. 7018, pp. 690–690, 2004.

[10] T. Cambau, J. Bico, and E. Reyssat, "Capillary rise between flexible walls," *EPL (Europhysics Letters)*, vol. 96, no. 2, p. 24001, 2011.

[11] Y. Di, X. Xu, and M. Doi, "Theoretical analysis for meniscus rise of a liquid contained between a flexible film and a solid wall," *EPL (Europhysics Letters)*, vol. 113, no. 3, p. 36001, 2016.

[12] S. Jahanshahi-Anbuhi, P. Chavan, C. Sicard, V. Leung, S. M. Z. Hossain, and R. Pelton, "Creating fast flow channels in paper fluidic devices to control timing of sequential reactions," *Lab on a Chip*, vol. 12, no. 23, pp. 5079–5085, 2012.

[13] L. J. Yang, T. J. Yao, Y. L. Huang, Y. Xu, and Y. C. Tai, "Marching velocity of capillary meniscuses in microchannels," *Proceedings of the IEEE Micro Electro Mechanical Systems (MEMS)*, pp. 93–96, 2002.

[14] E. Fu, S. A. Ramsey, P. Kauffman, B. Lutz, and P. Yager, "Transport in two-dimensional paper networks," *Microfluidics and Nanofluidics*, vol. 10, no. 1, pp. 29–35, 2011.

CONTACT

1. Sam Fishlock, tel +442890368433; s.fishlock@ulster.ac.uk
2. James McLaughlin +442890368933; jad.mclaughlin@ulster.ac.uk